

PLUS MODEL BASED LAND USE CHANGE ANALYSIS AND MULTI-SCENARIO SIMULATION FORECAST IN THE MIDDLE YELLOW RIVER HUANGFUCHUAN BASIN

WANG, L. X.¹ – LIU, Q.^{1,2*}

¹*College of Resources and Environmental Engineering, Tianshui Normal University, Tianshui
741000, China*

²*State Key Laboratory of Soil Erosion and Dryland Farming on Loess Plateau, Institute of Soil
and Water Conservation, Chinese Academy of Sciences and Ministry of Water Resources,
Yangling 712100, China*

**Corresponding author
e-mail: guangmingliu1983@163.com*

(Received 10th Jun 2024; accepted 18th Oct 2024)

Abstract. Climate change and human activity have led to substantial ecological degradation in the Yellow River Basin, China. As a case study, the aim of this study was to analyze and simulate current land-use status in the Huangfuchuan Basin from 1980 to 2020 and forecast multiple land-use scenarios in 2030 based on the patch-generating land use simulation (PLUS) model. The results showed that: (1) From 1980 to 2020, the average proportion of grassland, arable land, construction land, forest land, water area, and unused land in the total basin area was 66.16%, 21.17%, 0.97%, 4.96%, 2.08%, and 4.65%, respectively. Grassland and arable land remained as the primary land-use type, whereas construction land area showed continuous increase. (2) Annual precipitation and distance from the railway contributed the most to forest land expansion, whereas (in order) precipitation, altitude, and distance most strongly influenced water bodies and residential land. (3) The simulation forecast under the scenario of farmland protection showed that the cultivated land area will increase to 673.8 km² by 2030. In turn, the unused land area will increase by 31.8 km² but the grassland area will decrease by 49.4 km². In the ecological protection scenario, the area of arable land and forest land will increase, whereas that of grassland and water area will decrease by 6.9 and 0.72 km², respectively.

Keywords: *global environmental change; land-use planning; land-use planning; driving factor; ecological protection*

Introduction

The increasing rate of global environmental change and associated problems has led to the establishment of land use/cover change (LUCC) as a hot topic in academic research (Huang et al., 2024). LUCC objectively reflects the impact of natural and human factors on surface vegetation and dynamically shows the evolution of the Earth's surface landscape, thereby allowing the interaction mechanism between humans and the natural environment to serve as the basis for studying the consequent evolution process of the surface (Okembo et al., 2024a). Currently, LUCC is utilized for studying multiple critical issues including hydrology, ecological service value, climate change, and carbon balance (Zhang et al., 2024). Moreover, the Land Use and Land Cover Change Programme has been a joint initiative of the International Geosphere Biosphere and the International Human Factors Programme on Global Environmental Change since 1990 (Zhang et al., 2024).

Specifically, land use refers to the rational development and utilization of land resources by humans, whereas land cover is the surface cover formed under the

influence of natural and human factors including vegetation and buildings (Gao et al., 2024). Research on the scale of land-use change involves landforms such as river basins, as well as administrative areas such as the state (Tang et al., 2024), province, county, and city (Wang et al., 2024). As a vanguard for regional development (Singh et al., 2024), cities have played a substantial role in promoting land-cover changes in surrounding areas (Hu et al., 2024). Urban LUCC is affected by a variety of factors (Okembo et al., 2024b), which are mainly manifested as urban expansion and changes in adjacent land use patterns. Research involving specific landforms or regions primarily focuses on the characteristics of land use (Park et al., 2024), spatiotemporal changes in ecologically fragile areas, evaluation of ecological service value systems, driving factors affecting land-use type change, changes in land-use landscape patterns (Freire et al., 2024), and the dynamic simulation of ecological risk (Zhang and Atkinson, 2008). Notably, the development of geographic information systems (GIS) and remote sensing technology has facilitated the continual evolution of models related to land-use research. Representative quantitative prediction models include the Markov model and artificial neural network model (Cao and Li, 2023), with spatial prediction models including the cellular automata (CA), conversion of land use and its effects at small regional extent (CLUE-S), and future land use simulation (FLUS) models (Brackley et al., 2012). Alternatively, the patch-generating land use simulation (PLUS) model, based on the FLUS model, incorporates land-expansion analysis strategy (LEAS) and random seed CA modules to dynamically simulate the spatiotemporal generation of various land-use patches and effectively explain the factors affecting land use change with high precision (Huang et al., 2023). Combined with the evaluation of LUCC at different scales (Rodrigues et al., 2016), such as landform or administrative, the application of such models in simulating land-use change under multiple protection scenarios is expected to become the basis for future land-use planning (Zhong et al., 2023), which is of considerable significance for realizing the harmony and stability of the regional population, social economy, and ecology (Thomas et al., 2019). Compared with the above land use prediction models, the PLUS model can better excavate the incentives of various types of land use change, simulate the patch-level changes of multiple types of land use, and achieve the dual advantages of land use quantity and spatial structure prediction.

The Huangfuchuan River is a first-class tributary of the Yellow River, transporting 0.64×10^8 t of sediment to the Yellow River annually. However, the Huangfuchuan Basin has experienced substantial ecological degradation, and climate change and disorderly human activities have caused significant changes in ecosystem services in this area. Accordingly, the associated serious soil and water losses have become key areas of focus in the high-quality development strategy for the Yellow River Basin. In this context, the Huangfuchuan Basin in the middle reaches of the Yellow River was selected as the research object of this land-use study, with the aim of analyzing the spatiotemporal evolution characteristics of ecosystem services from 2000 to 2020 and identifying the expanded regions of ecosystem services. The PLUS model was used to simulate the spatial distribution pattern of the integrated ecosystem services under the scenarios of natural development, ecological protection, construction priority, and sustainable development in 2030. The combination and effect intensity of different ecosystem services were analyzed via superimposed expanded areas, and the land-use situation of the Huangfuchuan Basin in 2030 was predicted. Together, our findings

provide an informed basis to guide future land-use planning in this region to optimize land resources and land-use structures.

Materials and methods

Study area

The Huangfuchuan River Basin is located on the upper right bank of Hekou Town and Longmen District in the middle reaches of the Yellow River, between 110.3°–111.2° E and 39.2°–39.9° N, with a distance of 89.5 km from north to south and 102.1 km from east to west. It is a representative river of the main coarse sand area in the middle reaches of the Yellow River. The Huangfuchuan River originates from the Dianpan Gully in the northwest of Aobao Liang in the south of Dalat Banner, Inner Mongolia Autonomous Region, China, flows through the transitional zone of the Loess Plateau in Inner Mongolia and northern Shaanxi Province, and empties into the Yellow River in Fugu County, Shaanxi Province (*Fig. 1*). The basin has a high altitude in the northwest and a low altitude in the southeast, with the highest and lowest points at 1482 and 833 m above sea level, respectively. The river length is 137 km, and the basin area is 3246 km². The Huangfuchuan Basin is located in a semi-arid and sub-humid zone with a temperate continental monsoon climate. The flood season of river runoff is mainly from June to September. The vegetation in the basin is sparse, with the existing vegetation consisting mainly of grassland and forest land, and the soil types are mainly loess.

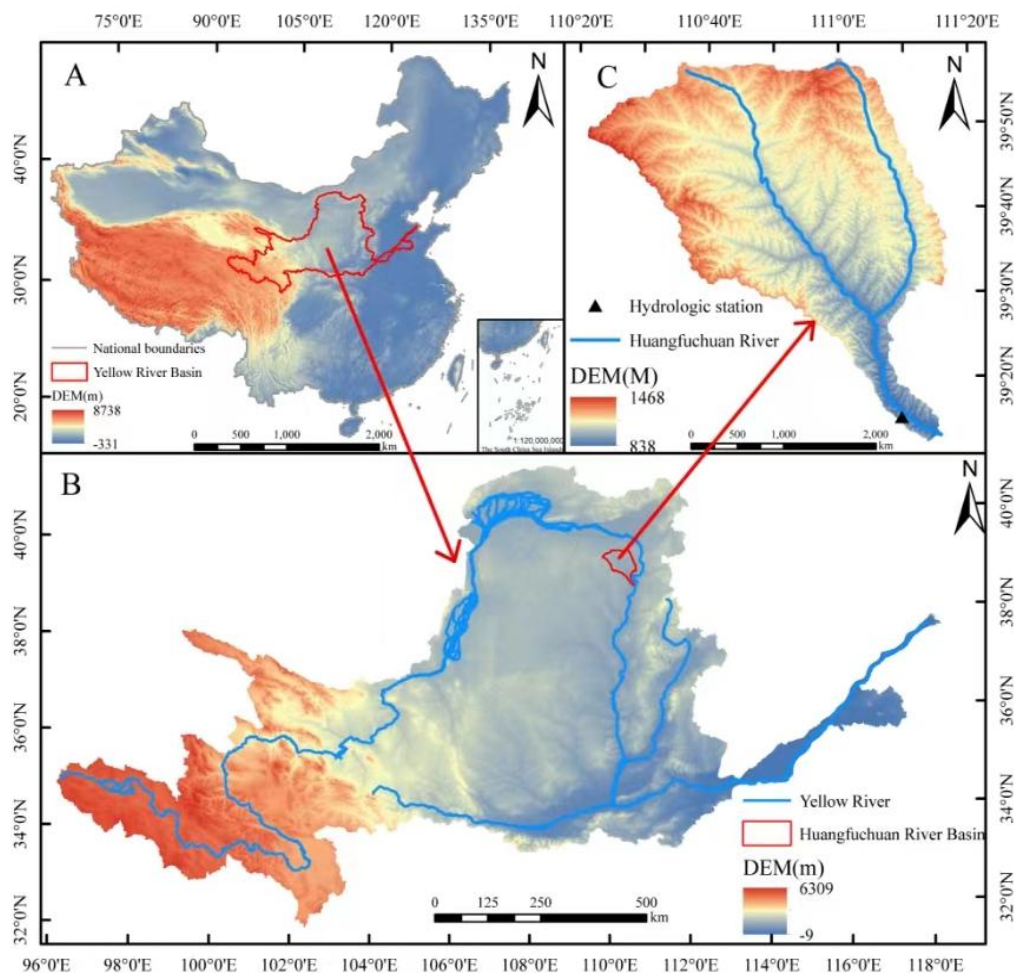


Figure 1. Maps displaying the location of the Huangfuchuan River Basin in China. Panels B and C represent the enlarged areas outlined in red in panels A and B, respectively. DEM, digital elevation model

Data sources

The data included natural, social, and accessibility data (Table 1). DEM data were derived from the geospatial data cloud platform (<https://www.gscloud.cn/>). Land-use, population density, gross domestic product (GDP), and natural factor data from 1980 to 2020 were derived from the Data Center for Resources and Environmental Sciences, Chinese Academy of Sciences (<https://www.resdc.cn/>), referring to the Chinese Multi-period Land use/Land Cover Remote Sensing Monitoring Data Classification system. Using the ArcGIS reclassification tool, the land use of the basin was divided into 21 categories of secondary types and six categories of primary types: grassland (high-, medium-, and low-coverage), cultivated land (paddy field and dry land), forest land (forest land, shrub land, sparse forest land, and other forest land), water (canals, lakes, reservoirs, and beaches), residential land (urban land, rural settlements, and other residential land), and unused land (sandy land, Gobi land, saline–alkali land, marshland, bare land). Social and economic factors such as the distance from the highway and railway and other data were from OpenStreetMap, utilizing the ArcGIS Euclidean distance tool to obtain the data (<https://www.openstreetmap.org/>).

Table 1. Data sources for driving factors for land-use change in the Huangfuchuan Basin

System attribute	Driving factor	Description	Unit
Natural environment	Elevation	Elevation value of each pixel	m
	Air temperature	Average annual temperature of each pixel	°C
	Precipitation	Average annual precipitation value of each pixel	mm
Social economy	GDP	GDP per pixel	Yuan/km ²
	Population density	Population density of each pixel	Person/km ²
Accessibility	Distance to the highway	Distance from the center of each pixel to the nearest road	m
	Distance to the railroad	Distance from the center of each pixel to the nearest railway	m

GDP, gross domestic product

Spatiotemporal pattern analysis of LUCC

Land use transfer matrix

The land use transfer matrix is a useful tool for analyzing LUCC over a certain period. It shows the change and transfer direction of the land-use type area at the beginning and end of the study period in the form of a matrix and serves as the basis for analyzing the structural change and transfer direction of the land-use type (Nie et al., 2023). The formula is as follows:

$$P = \begin{pmatrix} A_{11} & A_{12} & \dots & A_{1n} \\ A_{21} & A_{22} & \dots & A_{2n} \\ \vdots & \vdots & A_{ij} & \vdots \\ A_{n1} & A_{n2} & \dots & A_{nn} \end{pmatrix} \quad (\text{Eq.1})$$

where P is the land-use area, i and j are the land-use types at the beginning and end of the study, respectively, and n is the land-use type.

Land use dynamic attitude

Land-use dynamics are mainly used to represent the change in land-use type over a period of time; that is, the change rate of land use, which is divided into single and comprehensive land-use dynamic attitudes (Li et al., 2020). A single land-use dynamic attitude index K describes the change in the amplitude and speed of a certain land-use type at a specific time (Gong et al., 2023), and is calculated as follows:

$$K = \frac{U_{t2} - U_{t1}}{U_{t1}} \times \frac{1}{t_2 - t_1} \times 100\% \quad (\text{Eq.2})$$

where K is the dynamic attitude of a certain land use type in the study period, and U_{t1} and U_{t2} is the area of a certain land use type in the t_1 and t_2 periods, respectively.

The comprehensive land-use dynamic attitude index S reflects the comprehensive impact of human activities on various land-use types in the study area (Cherla et al., 2021). The calculation formula is as follows:

$$S = \frac{\sum_{i=1}^n |U_{t_2i} - U_{t_1i}|}{2 \times \sum_{i=1}^n U_{t_1i}} \times \frac{1}{t_2 - t_1} \times 100\% \quad (\text{Eq.3})$$

where S represents the dynamic attitude of a certain land use type during the study period. U_{t_1i} and U_{t_2i} are the beginning and end areas of the first land-use type during the t_1 and t_2 periods, respectively. The study period was 10,40, in units of years.

Comprehensive index of land-use degree

Land development is one way by which humans change land use. The comprehensive degree index of land use reflects the degree of human-derived change of regional land use, and can measure the breadth and depth of land use, with the degree of land use being divided into four indices. The classification index is divided into unused land (1); forest land, grassland, and water (2); cultivated land (3); and residential land (4). The degree of land development and utilization is proportional to this index (Koko et al., 2023).

The comprehensive index formula of land-use degree is as follows:

$$I = 100 \sum_{i=1}^n A_i D_i \quad (\text{Eq.4})$$

where I is the comprehensive index of land-use degree in the study area, A_i is the grade-level land-use degree classification index, and D_i is the percentage of area of Level land-use degree.

The formula of land use degree change is as follows:

$$\Delta I_{b-a} = I_b - I_a = \left(\sum_{i=1}^n A_i \times D_{ib} - \sum_{i=1}^n A_i \times D_{ia} \right) \times 100\% \quad (\text{Eq.5})$$

where, ΔI_{b-a} is the comprehensive change index of the land use degree, I_b and I_a are the comprehensive indices of the land use degree at corresponding times, and D_{ia} and D_{ib} are the area percentages of the corresponding time and grade of the land-use degree, respectively (Cherla et al., 2021).

PLUS model

PLUS model-based simulation incorporates LEAS and CA (CA based on multiple random seeds (CARS)) modules to effectively explain the factors affecting land-use change with high precision (Liu et al., 2023). The LEAS module utilizes the rule mining method to better explore the partial acquisition development probability of various types of land expansion and explore the driving force factors to determine the contribution of various types of land expansion during the study period (Palermo et al., 2021). Combining random seed generation and threshold decline mechanisms, the CA module can dynamically simulate the generation of various land-use patches in time and space (Penny et al., 2023). In the model, land quantity was predicted using the Markov model and data from existing years to predict the land quantity in 2030. First, the land-use expansion in 2020 was extracted using the PLUS model, and the development probability of various

types of land was obtained. The change in land-use type in the Huangfuchuan Basin in 2030 was simulated using the CA model of multiple random patch seeds. Second, natural and socioeconomic factors were identified as the main factors. Seven influencing factors, including elevation, precipitation, air temperature, population density, GDP, and distance from the highways and railways in the Huangfuchuan Basin were selected. After data raster processing, the spatial resolution and projection coordinate system were unified with the LUCC data. The LEAS module was then used to obtain the development probability of each land-use type in the study area. Finally, the baseline, cultivated land development, and ecological development scenarios were set according to the transfer cost matrix, neighborhood weight, target pixel number, and impact factors of various land-use types, and the development and change in land-use quantity in 2030 were comprehensively analyzed (Palermo et al., 2021).

Precision evaluation

Kappa and figure of merit (FOM) coefficients were used to evaluate the simulation accuracy of the model (Ma et al., 2023). The kappa coefficient was used to verify the data consistency based on the confusion matrix. Kappa is a statistical consistency indicator with a value between $[-1,1]$, usually > 0 . A kappa coefficient value > 0.7 indicates high consistency and accuracy of the simulation results (Table 2) (Gao et al., 2023). The formula is as follows:

$$Kappa = \frac{p_o - p_c}{p_p - p_c} \quad (Eq.6)$$

where the correct proportion of the grid is simulated under random and ideal states. The judgment criteria are listed in Table 2.

Table 2. Correspondence of the kappa coefficient to the simulation effect

Kappa coefficient	0–0.2	0.2–0.4	0.4–0.6	0.6–0.8	0.8–1
Simulation effect	Feeble	Weak	Moderate	Substantial	Optimum

Owing to the limitations of the kappa coefficient in consistency verification, the PLUS model provides the *FOM* coefficient on this basis. The *FOM* coefficient is an index for evaluating the simulation accuracy of the model and reflects the unity-level consistency and model-level similarity. The value of the coefficient is between 0.01 and 0.25; the higher the value, the higher the accuracy of the simulation results. The size of the index is affected by the number of simulation years, and an increase in the FOM index of ≤ 0.01 was taken as the standard level (Li et al., 2023). The formula is as follows:

$$FOM = B / (A + B + C + D) \quad (Eq.7)$$

The expression error area *A* predicts the persistence based on the observed change, the correct area *B* predicts the change based on the observed change, the wrong area *C* predicts the category obtained when the observed change predicts the error, and the error *D* predicts the change based on the observed persistence.

Land quantity forecasting

Scenario setting

To further explore the land-use type change in the Huangfuchuan Basin, the baseline, cultivated land protection, and ecological protection scenarios were established (see *Tables 2–4*). The cultivated land protection scenario was set based on the baseline scenario, and the Markov transfer probability matrix was modified to reduce the transfer probability of controlled cultivated land to residential land by 70% and to grassland and water by 40%. Alternatively, the probability of transferring unused land to cultivated land was increased by 50%. The cultivated land protection policy was strictly implemented. The ecological protection scenario was established to reduce the probability of converting forestland, grassland, and water into residential land by 60%. In addition, cultivated land has a certain ecological capacity. However, the probability of conversion from cultivated land to residential land was set to be reduced by 50%, with the reduced part being added to the probability of conversion from cultivated land to forest land. The probability of switching unused land to forest and grassland land was increased by 30% (Xu et al., 2023). In the land-use cost transfer matrix, 0 means that transformation is not allowed, and 1 means that transformation is allowed. In general, residential land cannot be easily transformed under ecological protection scenarios. The expansion intensity of land-use type is represented by domain weight (*Table 3*), which was determined according to expert experience and various model tests, or the weight value was calculated according to the proportion of the area expansion of each land-use type, and the domain effect generated by each land-use type was determined. The value was between [0,1], with the smaller the value, the smaller the influence of the neighborhood, and the weaker the expansion ability (Takahashi and Ihara, 2023a).

Markov quantity prediction

According to the land-use probability transfer matrix of the Huangfuchuan Basin from 2010 to 2020, a transfer cost matrix was established with regard to the three scenarios, and the migration and change in each land-use type in 2030 under the three scenarios were predicted (*Table 4*) (Takahashi and Ihara, 2023b).

Table 3. Neighborhood weights for each land use type

Land-use type	Cropland	Forest land	Grassland	Water	Residential land	Unused land
Cropland	1	1	1	1	1	1
Forest land	1	1	1	1	1	0
Grassland	1	1	1	1	1	1
Water	1	1	1	1	1	1
Residential land	1	1	1	1	1	1
Unused land	1	1	1	1	1	1
Neighborhood weight	0.046	0.001	0.445	0.009	0.106	0.394

Table 4. Cost matrix for land-use conversion in the three simulated scenarios

	Baseline scenario						Cultivated land protection scenario						Ecological protection scenario					
	a	b	c	d	e	f	a	b	c	d	e	f	a	b	c	d	e	f
a	1	1	1	1	1	1	1	1	1	1	0	1	1	1	1	1	0	1
b	1	1	1	1	1	0	1	1	1	1	1	0	1	1	1	1	0	0
c	1	1	1	1	1	1	1	1	1	1	0	1	1	1	1	1	0	1

d	1	1	1	1	1	1	1	1	1	1	1	1	1	1	1	1	0	1
e	1	1	1	1	1	1	1	1	1	1	1	1	1	1	1	1	1	1
f	1	1	1	1	1	1	1	1	1	1	1	1	1	1	1	1	1	1

a, b, c, d, e, and f represent cropland, forest land, grassland, water, residential land, and unused land, respectively; 0 indicates that conversion is not allowed, and 1 indicates that conversion is allowed. The rows represent roll-out, and the columns represent roll-in

Results

Spatiotemporal distribution of land use

The main land-use type in the Huangfuchuan Basin is grassland, with cropland being mainly distributed on both sides of the river and in low-lying areas (*Fig. 2*). Forest land is mainly distributed in the western and northeastern parts of the basin. In 1980, residential land was mainly distributed in the central and northern parts of the basin, with a discrete band distribution along the river. In 2020, residential land was concentrated mainly in the central part of the basin. From 1980 to 2020, the average proportions of grassland, croplands, residential land, forestland, water, and unused land were 66.16%, 21.17%, 0.97%, 4.96%, 2.08%, and 4.65%, respectively.

LUCC in the Huangfuchuan Basin during the past 40 years has been relatively large, with each land-use type having increased or decreased to different degrees. The areas of residential land, forestland, water and unused land increased by 17.36, 30.99, 6.54, and 20.12 km², respectively, reflecting 0.43% 0.77%, 0.16%, and 0.50% increases in the land-use ratios. The grassland and cropland areas decreased by 43.64 and 31.40 km², respectively, with grasslands showing the largest change rate overall with a decrease of 1.09% (*Table 5*).

Land use transfer matrix

Based on the superposition calculation and statistical analysis of the land-use classification results of the Huangfuchuan Basin for the five periods from 1980 to 2020, a transfer matrix between different land-use types was obtained (*Table 6*). Among the land use types, grassland was markedly degraded from 1980 to 2020, with 46.47 km² of grassland having been transformed into cropland and 35.10 km² transformed into unused land. Alternatively, 54.92 km² of cropland was transformed into grassland and 8.83 km² was transformed into water, representing the main transformation underlying water area increase. Compared to that in 1980, the area of residential land increased, mainly through the conversion of grassland and cropland.

The conversion to forest land area increased the most for grassland (28.43 km²), followed by cropland (11.54 km²), with the increase in forest land area steadily increasing under the measures of returning farmland to forest and afforestation (*Table 6*).

Table 5. Land use changes in the Huangfuchuan Basin from 1980 to 2020

Land-use type	1980		2020		Land-use change	
	Area km ²	Ratio %	Area km ²	Ratio %	Change/km ² km ²	Change rate %
Grassland	2122.50	66.50	2078.86	65.13	-43.64	-1.09
Cropland	691.57	21.67	660.16	20.68	-31.40	-0.79
Residential land	26.02	0.82	43.38	1.36	17.36	0.43

Forestland	145.50	4.56	176.49	5.53	30.99	0.77
Water	62.70	1.96	69.24	2.17	6.54	0.16
Unused land	143.37	4.49	163.49	5.12	20.12	0.50

Table 6. Transfer matrix of land-use change in the Huangfuchuan Basin from 1980 to 2020

Land type	Grassland	Cropland	Residential land	Forest land	Water	Unused
Grassland	1997.59	46.47	9.22	28.43	4.23	35.10
Cropland	54.92	604.87	5.40	11.54	8.83	5.31
Residential land	0.94	0.95	23.90	0.14	0.06	0.04
Forest land	6.76	2.04	1.20	134.60	0.22	0.62
Water	2.60	3.80	0.15	0.21	55.73	0.17
Unused	14.73	1.38	3.41	1.51	0.16	122.02

Characteristics of land use dynamic attitude change

From 1990 to 2000, the unused land area exhibited the fastest change (0.015%/a) for a single land-use type, followed by the water land area (0.008%/a). From 2000 to 2010, the unused land area decreased, with a single land-use dynamic attitude of $-0.023\%/a$. Residential land had the largest positive change (0.028%/a), followed by forest land (0.019%/a). Residential land also showed the highest value (0.029%/a) from 2010 to 2020, whereas unused land surface exhibited the largest change compared to that in the previous period (Fig. 3). During the 40-year period, residential land continued to increase, unused land showed the largest change, and the areas of forest land and water increased and decreased, whereas grassland and cropland land decreased. Cropland showed the least change between 1980 and 2020, with a single adjustment of $-0.005\%/a$ (Fig. 2). Among the dynamic attitudes of comprehensive land use during the study period, the largest land use change (0.036%/a) occurred from 2010 to 2020 (Fig. 4).

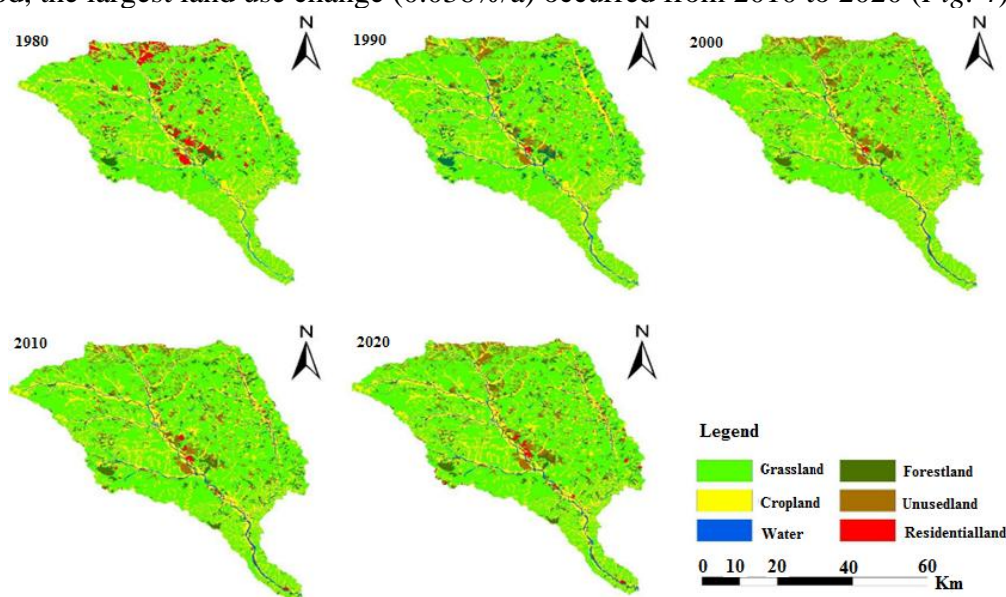


Figure 2. Distribution of land-use types in the Huangfuchuan Basin from 1980 to 2020

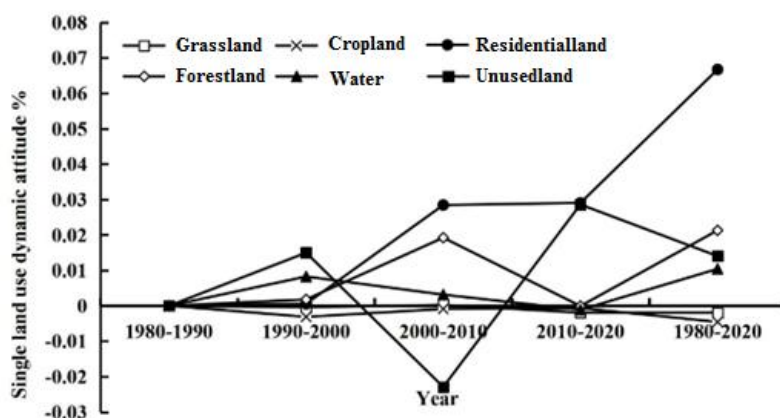


Figure 3. Changes of single land-use dynamic attitude in the Huangfuchuan Basin from 1980 to 2020

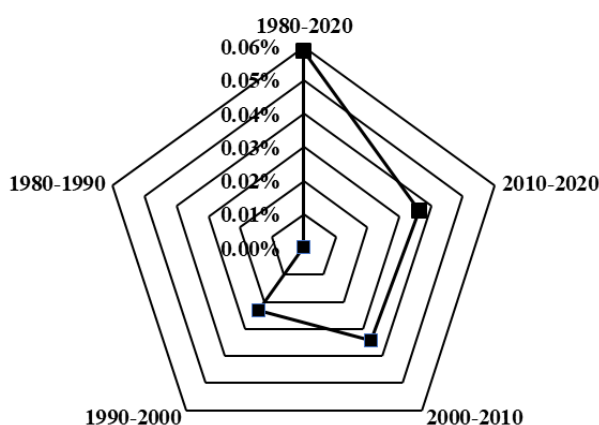


Figure 4. Changes of integrated land-use dynamic attitude in the Huangfuchuan Basin from 1980 to 2020

Calculation of the comprehensive index of land-use degree revealed that this metric fluctuated between 217.48 and 218.94 from 1980 to 2020 (Table 7), with a generally declining trend. This indicated that the land use level of the Huangfuchuan Basin was slightly reduced, and the utilization efficiency of land resources was not high.

Table 7. Comprehensive index of land use degree in the Huangfuchuan Basin, 1980–2020

Year	Comprehensive index of land use degree	Variation	Rate of change %
1980	218.81	—	—
1990	218.82	0.0084	0.0008
2000	217.48	1.3388	0.1339
2010	218.94	1.4630	0.1463
2020	218.28	0.6589	0.0659
1980–2020	—	—	0.3469

“—” indicates no available data

Driving force analysis of land-use change in the Huangfuchuan Basin based on the PLUS model

The PLUS model was used to analyze the driving forces of land expansion by land-use type in the Huangfuchuan Basin from 1980 to 2020, revealing that the root-mean-square error of the driving force for the expansion of forest land, water, residential land, and unused land was less than 0.15. In comparison, the errors for cropland and forest land were > 0.167 , and the overall effect was better. As shown in *Figure 5*, the driving factors affecting the contribution of crop land to the highest degree were the annual average temperature, annual precipitation, and distance from the highway. Annual precipitation and distance from the railway contributed the most to forest land expansion. The highest contributions of water and residential land were mediated by precipitation, elevation, and distance from the highway. Population density was the most important factor contributing to the expansion of unused land. As shown in *Figure 6*, both forestland and water expansion occurred on the clear dividing line of precipitation. Cropland expansion was mainly affected by temperature, with the expansion scope of cropland being large and dispersed, whereas grassland and unused land expansion were related to population density. The areas of grassland and unused land with a high population density were relatively small, and the areas with significant residential land expansion were close to roads.

Verification of PLUS model accuracy

To verify the simulation accuracy of the constructed PLUS model, land-use type data for 2010 and 2020 were used to simulate the spatial distribution of land use in the Huangfuchuan Basin in 2020. By resampling the land-use data for 2020, a confusion matrix was established between the actual and simulated values. The kappa, overall accuracy, and *FOM* coefficients were calculated. The model simulation results showed that the actual value of the land-use type in 2020 was close to the simulated value. The kappa coefficient obtained by the test calculation was 0.858, and the overall accuracy was 0.925, which was between [0.8, 1] and represented the best simulation effect. For the *FOM* coefficients, $A = 174,694$, $B = 15,779$, $C = 1625$, and $D = 88,225$, the calculated *FOM* coefficient was 0.056, and the producer accuracy was 0.082. The results showed that the PLUS model is suitable for simulating the spatial distribution of land use in the Huangfuchuan Basin during this period and that the simulated development probability of each type of land use reached a relatively significant development result.

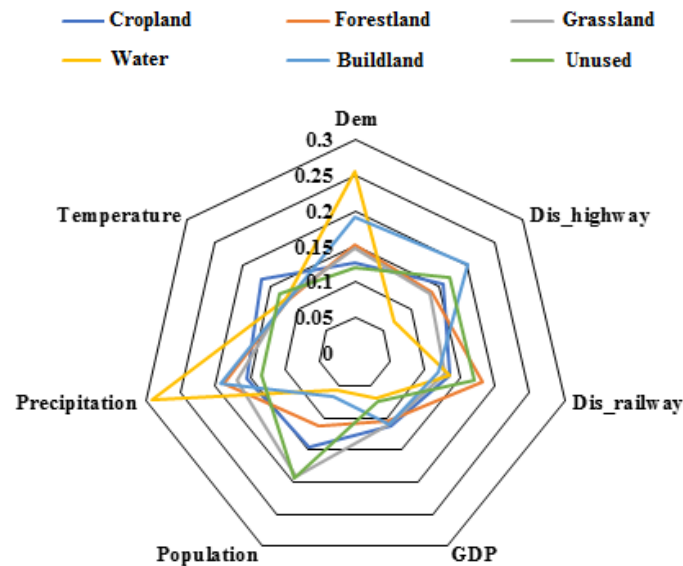


Figure 5. Contribution degree of driving factors for land expansion of various land-use types

Simulation forecast of land use status in 2030

Baseline scenario

As shown in *Figure 7*, under the baseline scenario, the areas of unused land, residential land, and forest land in the Huangfuchuan Basin were predicted to increase in 2030 compared to those in 2020, with the area of unused land increasing to 196.01 km². The projected area of residential land increased by 8.58 km² compared with that in 2020, and the area of forest land changed to 176.48 km², an increase of approximately 0.02 km². The cropland, grassland, and water areas were expected to decrease to varying degrees by 2030. Specifically, the area of grassland will be reduced to 2041.76 km², 36.39 km² less than that in 2020, representing largest type of land transferred out. In turn, the water and cropland areas will decrease by 0.68 and 4.12 km², respectively (*Table 8*).

Table 8. Land use status of the Huangfuchuan Basin in 2030 under three scenarios.

Scenario category	Cropland	Forest land	Grassland	Water	Residential land	Unused land
Current area in 2020/km ²	659.68	176.46	2078.15	69.24	43.30	163.43
Baseline scenario in 2030/km ²	655.56	176.48	2041.76	68.55	51.88	196.01
Cropland conservation in 2030/km ²	673.75	176.48	2028.75	67.13	48.89	195.24
Ecological protection by 2030/km ²	664.13	181.46	2071.21	68.52	48.68	163.71
Change rate of natural development in 2030	-0.62%	0.01%	-1.75%	-0.99%	19.83%	19.93%
Change rate of cropland protection in 2030	2.13%	0.01%	-2.38%	-3.04%	12.91%	19.46%
Change rate of ecological protection in 2030	0.68%	2.84%	-0.33%	-1.04%	12.45%	0.17%

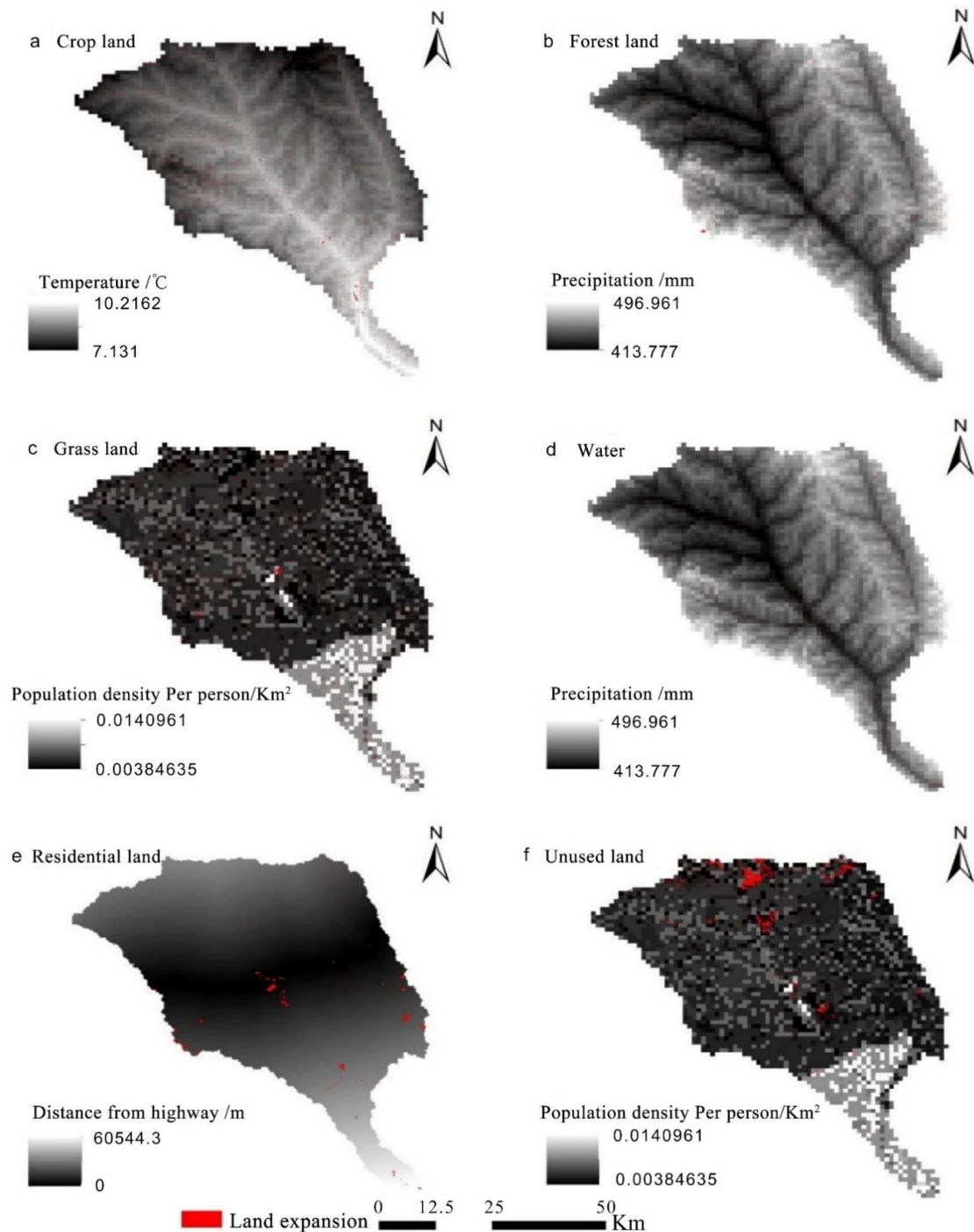


Figure 6. Overlay of class expansion and its main driving factors in various regions from 1980 to 2020

Cropland conservation scenario

In the context of protecting cultivated land, the probability of cultivated land being transferred to construction land is reduced by 70%, while the probability of being transferred to grassland and water areas is lowered by 40%. At the same time, the probability of uncultivated land being transferred to cultivated land is increased by 50%.

The calculation results show that the area of construction land will increase by 5.59 km² by 2030, which is significantly smaller than the change under the natural development scenario. By 2030, the cultivated land area will reach 673.75 km², an increase of 14.07 km² compared with the data in 2020; the grassland area will decrease by 49.40 km², while the uncultivated land area will increase by 31.81 km². Under the scenario of protecting cultivated land, the probability of cultivated land being transferred out is effectively controlled, thereby ensuring food security and grain production.

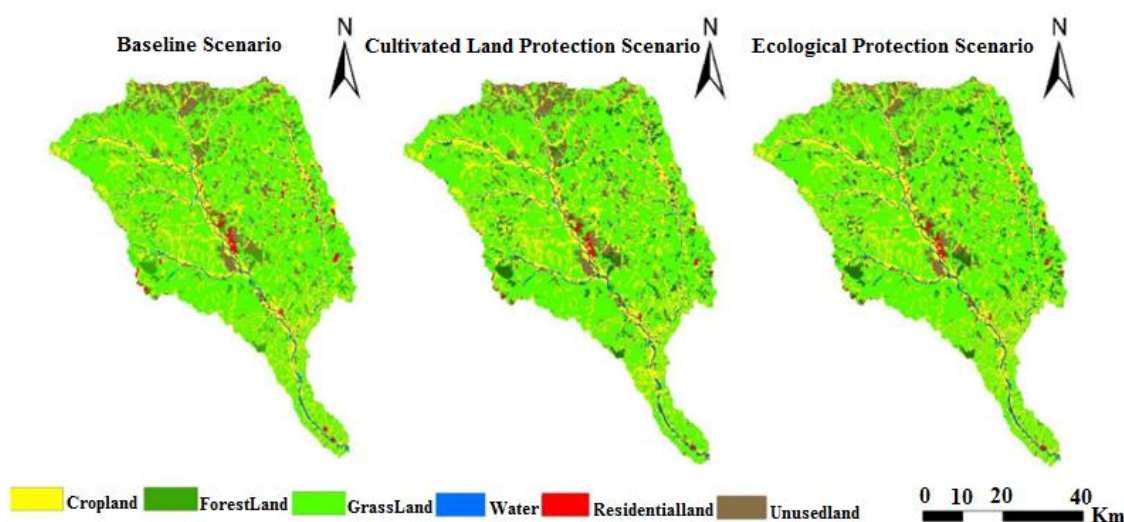


Figure 7. 2030 land-use simulation spatial distribution map of the Huangfuchuan Basin under the three scenarios.

Ecological protection scenario

Clear requirements have been proposed for the ecological protection and management of the Yellow River Basin, to which the Huangfuchuan Basin contributes. The development of various land types in the basin should be promoted, from excessive intervention and utilization to natural restoration and improvement of the high-quality ecology of the basin, building an ecological security pattern, and protecting the boundary of natural ecological security. Toward this end, under the ecological protection scenario, the conversion probability of forest land, grassland, and water to residential land was reduced, whereas that of unused land to forest land and grassland land was increased. PLUS modeling revealed that the area of cropland and forest land in 2030 will increase by 4.46 and 5 km², respectively, compared to that in 2020, whereas the area of residential land will increase by 5.39 km². However, the area of unused land was predicted to remain stable, whereas the grassland area will decrease by 6.94 km². The overall predicted change in land-use area by 2030 was small, indicating that the ecological environment is relatively stable under the implementation of and protection by the relevant policies (*Table 8*).

Discussion

Through the analysis of land-use change in the Huangfuchuan Basin from 1980 to 2020, it was found that with the acceleration of the urbanization process and the rapid

expansion of residential land in the basin, a large quantity of cultivated land was occupied, and the area of ecological land, such as forest land and grassland, was gradually degraded. By resampling the land-use data for 2020, a confusion matrix was established between the actual and simulated values. The kappa, overall accuracy, and *FOM* coefficients were calculated. The model simulation results showed that the actual value of the land-use type in 2020 was close to the simulated value. The kappa coefficient obtained by the test calculation was 0.858, and the overall accuracy was 0.925, which was between [0.8, 1] and represented the best simulation effect. For the *FOM* coefficients, $A = 174,694$, $B = 15,779$, $C = 1625$, and $D = 88,225$, the calculated *FOM* coefficient was 0.056, and the producer accuracy was 0.082. The results showed that the PLUS model is suitable for simulating the spatial distribution of land use in the Huangfuchuan Basin during this period and that the simulated development probability of each type of land use reached a relatively significant development result.

Therefore, if no effective farmland or ecological protection measures are established in the Huangfuchuan Basin in the future, construction land will occupy a large amount of arable land and ecological land space (Waidler et al., 2022). This situation will not only have a negative impact on ecological space protection, but also does not meet the requirements of the Chinese national policy of “clear water and green mountains” (Liu et al., 2022). In addition, such a development model cannot meet the needs of food security or promote the long-term goals of ecological civilization (Xu et al., 2022a). Accordingly, in future land-use planning, the focus should be on solving the contradiction between the supply and demand of construction and arable land while simultaneously paying attention to protecting the space and ecological function of ecological land (Cao et al., 2022).

The baseline, cultivated land, and protection scenarios correspond to different development orientations in the Huangfuchuan Basin from 1980 to 2020. Under the baseline scenario, unused land and residential land areas markedly increased, whereas forest land area showed little change. Under the ecological protection and baseline scenarios, the cropland area decreased (Hong et al., 2022). Under the cultivated and protected scenarios, the transfer area of grassland was the largest, whereas the increase in residential land area was the smallest (Li et al., 2022). Under the baseline and protection scenarios, the cropland area increased the most. In the ecological protection scenario, the unused land increased the least and grassland area decreased the least, compared with that in the baseline scenario. Forestland area increased the most under all three scenarios (He et al., 2022). Comprehensive comparison of the predicted change amplitude of different land-use types in 2030 under the three scenarios revealed the need to implement a cropland protection system and strengthen food security with the goal of protecting the quantity and quality of cropland (Lechner and Kirisits, 2022). Moreover, it is necessary to consolidate existing results in terms of ecology, implement ecological protection policies, strengthen ecological protection, and prevent the deterioration of the ecological environment in the basin (Getachew and Manjunatha, 2022). The ecosystem in the Huangfuchuan Basin is fragile and highly dependent on the inflow of external substances to maintain stability, with the dominant landscape being repressed (Xu et al., 2022b). When the external supply is insufficient, the ecosystem will collapse [48,49]. In addition, with the rapid development of cities within the basin, the increasing demand for external land and materials will put pressure on surrounding areas, reduce the level and diversity of ecosystem services, and indirectly affect the ecological functions of the basin (Xu et al., 2022).

In the three scenarios, land use efficiency in the land conservation scenario and ecological conservation scenario is significantly higher than that in the natural development scenario. Taking land conservation measures can align with the national policy of protecting farmland, which is beneficial to maintaining economic benefits and improving land use efficiency. In the ecological conservation scenario, better protection of forest and grassland ecological land can be achieved, but the intensity of farmland protection is insufficient. Taking into account the three scenarios, the future development of Huangfu River Basin should focus on sustainable land use to enhance regional carbon storage. Firstly, the protection of forestland and grassland, etc. should be strengthened to consolidate the ecological benefits brought by the implementation of the policy of returning farmland to forest and grassland. Secondly, the red line of farmland protection and the development boundary of towns and villages should be strictly delineated, and the underdeveloped land should be developed and utilized to avoid the loss of carbon storage caused by the encroachment of built-up land on farmland. At the same time, attention should be paid to the transfer of land categories between the interlaced areas of farmland, forestland, and grassland, appropriately increasing the area of forestland, optimizing the vegetation structure of forestland, and promoting the sustainable development of the watershed.

The Huangfu River Basin, as a key ecological construction area in China, should prioritize ecological protection while improving the efficiency of land use for construction purposes. It should also enhance the concentration of urban space and promote the coordinated development of ecological protection and economic construction. The continuous reduction of cultivated land in the Huangfu River Basin under ecological governance measures is not conducive to the improvement of ecological functions such as food production, raw material production, and nutrient cycling. In the future, the red line of cultivated land should be strictly guarded to ensure the safety of cultivated land. At the same time, efforts should be made to protect and restore grasslands and wetlands to maintain the stable enhancement of gas regulation and climate regulation functions. The land use structure in the Huangfu River Basin is quite different, leading to obvious differences in ecological value. Different places should implement targeted measures under the guidance of policies, fully considering local natural environment and human factors, consolidating the achievements of previous governance, and continuously promoting ecological construction. In summary, the overall ecological quality of the Huangfu River Basin has improved, but due to the fragility of the river basin's ecology and the trend of global ecological change, the recovery of ecological conditions is slow, and the environmental quality still poses a threat. The ecological governance and protection in the area are still a long way to go.

Conclusions

(1) Analysis of the temporal and spatial changes of land use in the Huangfuchuan Basin from 1980 to 2020 revealed that the comprehensive dynamic attitude of land use was 0.059%, with the land-use types mainly comprising grassland and cropland, accounting for 87.33% of the total area of the basin. The average proportions of forest land, water, grassland, cropland, residential land, and unused land were 4.96%, 2.08%, 66.16%, 21.17%, 0.97%, and 4.65%, respectively. Grassland area exhibited the greatest change and was the main type of land-use change.

(2) From 1980 to 2020, the area of land-use type in the Huangfuchuan Basin with the largest change was grassland, which decreased by 43.5 km², followed by cropland area, which decreased by 31.4 km². Conversely, forest land area showed the largest expansion, with the transferred area being approximately 41.8 km², representing an increase of 30 km² compared with that 1980. The area of water expansion changed the least, increasing by approximately 6.7 km². Except for grassland and cropland, the areas of the other four types of land use consistently increased; nevertheless, grassland consistently occupied the main position in the land-use structure of the basin.

(3) The PLUS model was used to analyze various factors of land-use expansion in the study area, and the accuracy of the model was verified by simulation. Multi-scenario simulation analyses were applied for predicting land use in 2030, which demonstrated that the PLUS model had good performance with regard to analyzing the driving forces of the expansion of various land-use types in the Huangfuchuan Basin from 1980 to 2020. The driving factors affecting cropland expansion were mainly temperature and precipitation, whereas that affecting forest land and water expansion was precipitation. The distance from highways and elevation were the main factors affecting residential land.

(4) The ecological protection scenario was optimal with regard to future land-use changes in the Huangfuchuan Basin. In the future, soil conservation and upgrading and protection of the water resource supply should be adopted for land use in the Huangfuchuan Basin to guarantee normal ecosystem operations. Overall, our results highlight soil and water conservation, led by ecological environmental management, as important for the protection of the Huangfuchuan watershed.

Acknowledgments. Many thanks to Min Du for their technical assistance in the laboratory work. We would like to thank Yiting Shao and Runze Liu for providing statistics assistance.

Funding. This research was supported by the Research Projects in Philosophy and Social Sciences of Gansu Province, China (2024YB105).

Conflict of interests. The authors declare no conflicts of interests.

REFERENCES

- [1] Brackley, C. A., Broomhead, D. S., Romano, M. C., Thiel, M. (2012): A max-plus model of ribosome dynamics during mRNA translation. – *Journal of Theoretical Biology* 303: 128-140.
- [2] Cao, J., Li, T. (2023): Analysis of spatiotemporal changes in cultural heritage protected cities and their influencing factors: evidence from China. – *Ecological Indicators* 151: 110327.
- [3] Cao, X., Liu, Z., Li, S., Gao, Z. (2022): Integrating the ecological security pattern and the PLUS model to assess the effects of regional ecological restoration: a case study of Hefei City, Anhui Province. – *International Journal of Environmental Research and Public Health* 19.
- [4] Cherla, A., Howard, N., Mossialos, E. (2021): The ‘Netflix plus model’: can subscription financing improve access to medicines in low- and middle-income countries? – *Health Economics Policy and Law* 16: 113-123.
- [5] Freire, T., Hu, Z., Wood, K. B., Gjini, E. (2024): Modeling spatial evolution of multi-drug resistance under drug environmental gradients. – *PLoS Computational Biology* 20: e1012098.

- [6] Gao, F., Xin, X., Song, J., Li, X., Zhang, L., Zhang, Y., Liu, J. (2023): Simulation of LUCC dynamics and estimation of carbon stock under different SSP-RCP scenarios in Heilongjiang Province. – *Land* 12: 1665.
- [7] Gao, J., Gong, J., Li, Y., Yang, J., Liang, X. (2024): Ecological network assessment in dynamic landscapes: multi-scenario simulation and conservation priority analysis. – *Land Use Policy* 139: 107059.
- [8] Getachew, B., Manjunatha, B. R. (2022): Impacts of land-use change on the hydrology of Lake Tana Basin, Upper Blue Nile River Basin, Ethiopia. – *Global Challenges* 6.
- [9] Gong, J., Du, H., Sun, Y., Zhan, Y. (2023): Simulation and prediction of land use in urban agglomerations based on the PLUS model: a case study of the Pearl River Delta, China. – *Frontiers in Environmental Science* 11.
- [10] He, Y., Mu, X., Jiang, X., Song, J. (2022): Runoff variation and influencing factors in the Kuye River Basin of the Middle Yellow River. – *Frontiers in Environmental Science* 10.
- [11] Hong, C., Zhao, H., Qin, Y., Burney, J. A., Pongratz, J., Hartung, K., Liu, Y., Moore, F. C., Jackson, R. B., Zhang, Q., Davis, S. J. (2022): Land-use emissions embodied in international trade. – *Science* 376: 597-603.
- [12] Hu, Z., Song, G., Hu, Z., Fang, J. (2024): An improved dynamic game analysis of farmers, enterprises and rural collective economic organizations based on idle land reuse policy. – *Land Use Policy* 140: 107098.
- [13] Huang, C., Zhou, Y., Wu, T., Zhang, M., Qiu, Y. (2024): A cellular automata model coupled with partitioning CNN-LSTM and PLUS models for urban land change simulation. – *Journal of Environmental Management* 351: 119828.
- [14] Huang, T., Wang, Z., Wu, Z., Xiao, P., Liu, Y. (2023): Attribution analysis of runoff evolution in Kuye River Basin based on the time-varying Budyko framework. – *Frontiers in Earth Science* 10.
- [15] Koko, A. F., Han, Z., Wu, Y., Zhang, S., Ding, N., Luo, J. (2023): Spatiotemporal analysis and prediction of urban land use/land cover changes using a cellular automata and novel patch-generating land use simulation model: a study of Zhejiang Province, China. – *Land* 12: 1525.
- [16] Lechner, C., Kirisits, C. (2022): The effect of land-use categories on traffic noise annoyance. – *International Journal of Environmental Research and Public Health* 19.
- [17] Li, K., Feng, M., Biswas, A., Su, H., Niu, Y., Cao, J. (2020): Driving factors and future prediction of land use and cover change based on satellite remote sensing data by the LCM model: a case study from Gansu Province, China. – *Sensors* 20: 2757.
- [18] Li, R., Zhao, X., Tian, Y., Shi, Y., Gu, X., Wang, S., Zhang, R., An, J., Su, L., Wang, X. (2023): Different responses of Japanese encephalitis to weather variables among eight climate subtypes in Gansu, China, 2005-2019. – *BMC Infectious Diseases* 23: 114.
- [19] Li, X., Liu, Z., Li, S., Li, Y. (2022): Multi-scenario simulation analysis of land use impacts on habitat quality in Tianjin based on the PLUS model coupled with the InVEST model. – *Sustainability* 14: 6923.
- [20] Liu, Q., Yu, F., Mu, X. (2022): Evaluation of the ecological environment quality of the Kuye River source basin using the remote sensing ecological index. – *International Journal of Environmental Research and Public Health* 19: 12500.
- [21] Liu, Y., Jing, Y., Han, S. (2023): Multi-scenario simulation of land use/land cover change and water yield evaluation coupled with the GMOP-PLUS-InVEST model: a case study of the Nansi Lake Basin in China. – *Ecological Indicators* 155: 110926.
- [22] Ma, G., Li, Q., Zhang, J., Zhang, L., Cheng, H., Ju, Z., Sun, G. (2023): Simulation and analysis of land-use change based on the PLUS model in the Fuxian Lake Basin (Yunnan–Guizhou Plateau, China). – *Land* 12: 120.
- [23] Nie, W., Xu, B., Yang, F., Shi, Y., Liu, B., Wu, R., Lin, W., Pei, H., Bao, Z. (2023): Simulating future land use by coupling ecological security patterns and multiple scenarios. – *Science of the Total Environment* 859: 160262.

- [24] Okembo, C., Morales, J., Lemmen, C., Zevenbergen, J., Kuria, D. (2024): A Land administration data exchange and interoperability framework for Kenya and its significance to the sustainable development goals. – *Land* 13: 435.
- [25] Palermo, T., Prencipe, L., Kajula, L. (2021): Effects of government-implemented cash plus model on violence experiences and perpetration among adolescents in Tanzania, 2018–2019. – *American Journal of Public Health* 111: 2227-2238.
- [26] Park, S. S., Lee, Y. K., Choi, Y. W., Lim, S. B., Park, S. H., Kim, H. K., Shin, J. S., Kim, Y. H., Lee, D. H., Kim, J. H., Park, T. J. (2024): Cellular senescence is associated with the spatial evolution toward a higher metastatic phenotype in colorectal cancer. – *Cell Reports* 43: 113912.
- [27] Penny, J., Ordens, C. M., Barnett, S., Djordjević, S., Chen, A. S. (2023): Small-scale land use change modelling using transient groundwater levels and salinities as driving factors – An example from a sub-catchment of Australia’s Murray-Darling Basin. – *Agricultural Water Management* 278: 108174.
- [28] Rodrigues, N. C., Lino, V. T., Dumas, R. P., Andrade, M. K., O’Dwyer, G., Monteiro, D. L., Gerardi, A., Fernandes, G. H., Ramos, J. A., Ferreira, C. E., Leite, I. D. (2016): Temporal and spatial evolution of dengue incidence in Brazil, 2001-2012. – *PLoS One* 11: e165945.
- [29] Singh, P., Fu, N., Dale, S., Orzol, S., Laird, J., Markovitz, A., Shin, E., O’Malley, A. S., McCall, N., Day, T. J. (2024): The comprehensive primary care plus model and health care spending, service use, and quality. – *JAMA - Journal of the American Medical Association* 331: 132-146.
- [30] Takahashi, T., Ihara, Y. (2023): Spatial evolution of human cultures inferred through Bayesian phylogenetic analysis. – *Journal of the Royal Society Interface* 20: 20220543.
- [31] Tang, H., Halike, A., Yao, K., Wei, Q., Yao, L., Tuheti, B., Luo, J., Duan, Y. (2024): Ecosystem service valuation and multi-scenario simulation in the Ebinur Lake Basin using a coupled GMOP-PLUS model. – *Scientific Reports* 14: 5071.
- [32] Thomas, S., Reynolds, D., Morrall, M., Limond, J., Chevignard, M., Calaminus, G., Poggi, G., Bennett, E., Frappaz, D., Slade, D., Gautier, J., McQuilton, P., Massimino, M., Grundy, R. (2019): The European Society of Paediatric Oncology Ependymoma-II program Core-Plus model: development and initial implementation of a cognitive test protocol for an international brain tumour trial. – *European Journal of Paediatric Neurology* 23: 560-570.
- [33] Waidler, J., Gilbert, U., Mulokozi, A., Palermo, T. (2022): A “Plus” model for safe transitions to adulthood: impacts of an integrated intervention layered onto a national social protection program on sexual behavior and health seeking among Tanzania’s youth. – *Studies in Family Planning* 53: 233-258.
- [34] Wang, S., Zhai, C., Zhang, Y. (2024): Evaluating the impact of urban digital infrastructure on land use efficiency based on 279 cities in China. – *Land* 13: 404.
- [35] Xu, F., Li, P., Chen, W., He, S., Li, F., Mu, D., Elumalai, V. (2022): Impacts of land use/land cover patterns on groundwater quality in the Guanzhong Basin of northwest China. – *Geocarto International* 37: 16769-16785.
- [36] Xu, L., Liu, X., Tong, D., Liu, Z., Yin, L., Zheng, W. (2022): Forecasting urban land use change based on cellular automata and the PLUS model. – *Land* 11: 652.
- [37] Xu, X., Wang, C., Wang, P., Chu, Y., Guo, J., Bo, X., Lin, A. (2023): Bioaerosol dispersion and environmental risk simulation: method and a case study for a biopharmaceutical plant of Gansu Province, China. – *Science of the Total Environment* 860: 160506.
- [38] Zhang, J., Wang, J., Zhao, N., Shi, J., Wang, Y. (2024a): Analysis of changes in runoff and sediment load and their attribution in the Kuye River Basin of the Middle Yellow River based on the slope change ratio of cumulative quantity method. – *Water* 16: 944.
- [39] Zhang, P., Atkinson, P. M. (2008): Modelling the effect of urbanization on the transmission of an infectious disease. – *Mathematical Biosciences* 211: 166-185.

- [40] Zhang, Z., Li, X., Liu, X., Zhao, K. (2024b): Dynamic simulation and projection of land use change using system dynamics model in the Chinese Tianshan mountainous region, central Asia. – *Ecological Modelling* 487: 110564.
- [41] Zhong, Y., Zhang, X., Yang, Y., Xue, M. (2023): Optimization and simulation of mountain city land use based on MOP-PLUS model: a case study of Caijia Cluster, Chongqing. – *ISPRS International Journal of Geo-Information* 12: 451.